Chu Figure S1

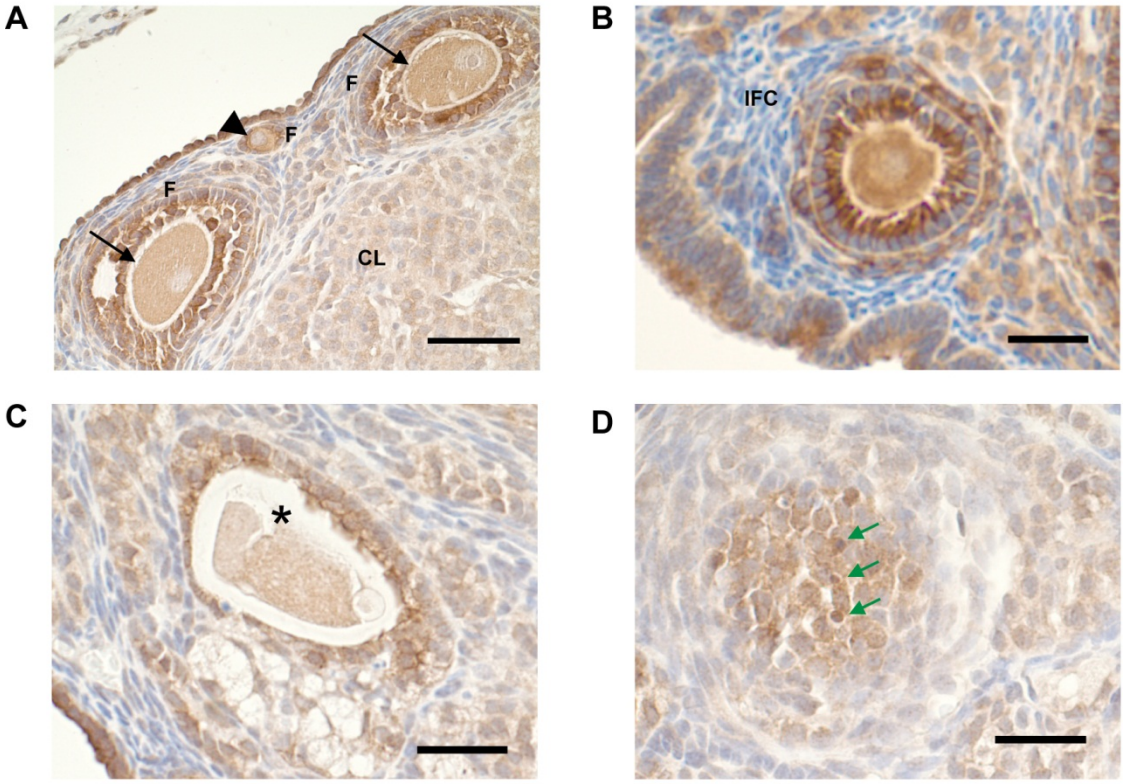

E

The relative intensity of p-eEF2 immunostaining in mouse ovarian cells

Follicular stages	Oocytes	Granulosa cells	Theca interna cells
Primordial and primary follicles	+	+	n/a
Small preantral follicles	++	+++	n/a
Large preantral follicles	++	+++	+
Small antral follicles	++	+++	+
Large antral follicles	+	+++	+
Corpora lutea	n/a	+	n/a

Figure S1. Phosphorylation of p-eEF2 in ovaries, related to Figure 1. (A-D) Immunostaining of p-eEF2 in 6-month old wild-type ovaries. **(A)** p-eEF2 was localized in different staged follicles (F) and corpora lutea (CL). The black arrowhead indicates a primordial follicle that transitioned to a primary follicle. The black arrows indicate oocytes. Scale bars represent 50 μm. **(B)** p-eEF2 staining was intense in granulosa cells near oocytes. Interfollicular stromal cells (IFC) were negative for p-eEF2 staining. Scale bars represent 20 μm. (**C,D)** Staining of p-eEF2 in atretic follicles. The black star indicates the degenerated oocyte in a late stage atretic follicle. The green arrows indicate granulosa cells with pyknotic nuclei that have intense p-eEF2 staining. Scale bars represent 25 μm. **(E)** The intensity of p-eEF2 immunostaining in mouse ovarian cells at different stages of follicle development. (+) relative-weak staining. (++) relative-strong staining. (+++) intense staining. (N/A) staining not analyzed.

Chu Figure S2

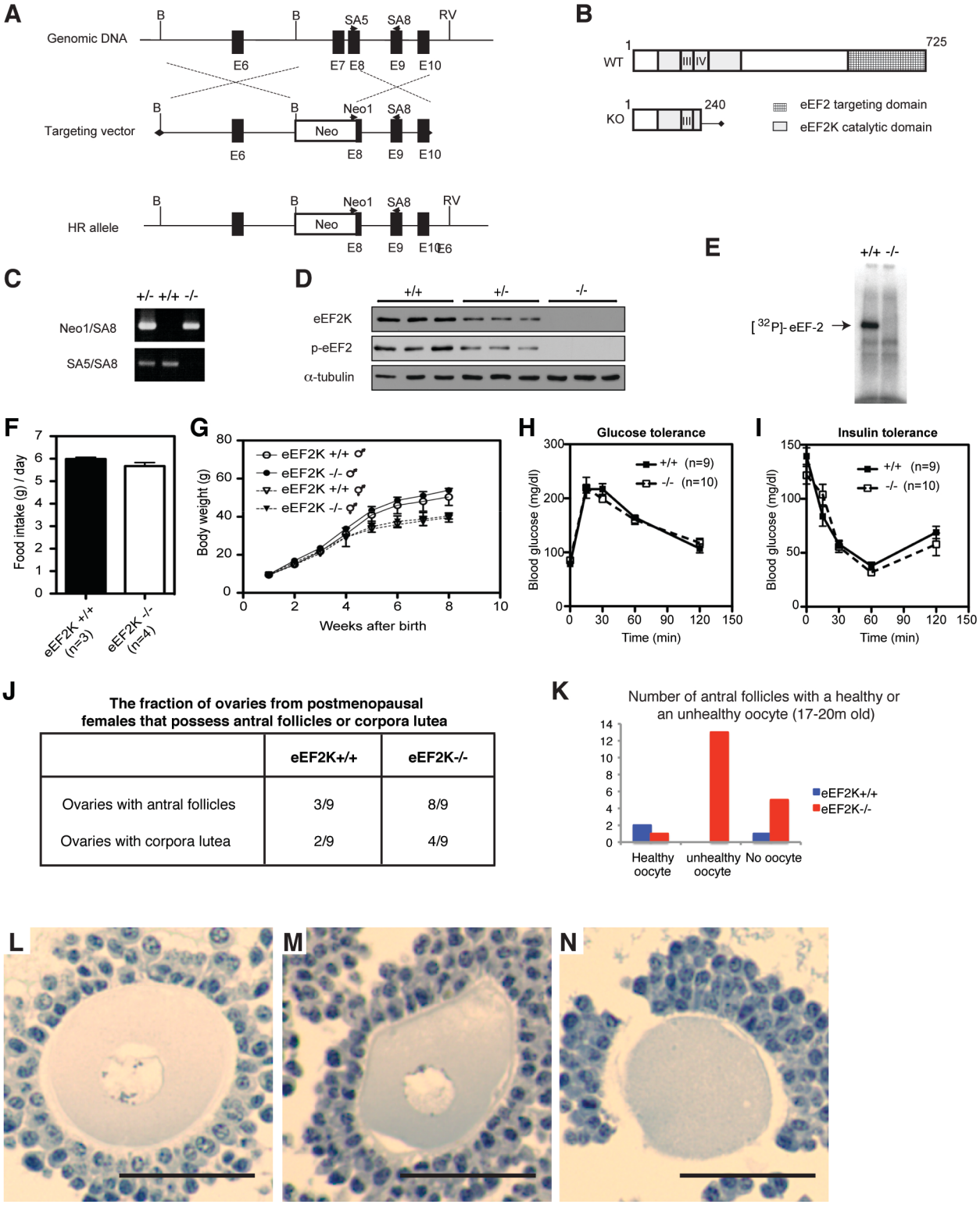

J

The fraction of ovaries from postmenopausal females that possess antral follicles or corpora lutea

	eEF2K+/+	eEF2K-/-
Ovaries with antral follicles	3/9	8/9
Ovaries with corpora lutea	2/9	4/9

Figure S2. Knockout of eEF2K leads to complete loss of eEF2 phosphorylation in mice, and the accumulation of unhealthy oocytes in eEF2K-/- aged mice, related to Figures 2 and 3. **(A,B)** Schematic representation of eEF2K knockout constructs. eEF2K-/- mice were generated using a targeting vector to delete exons 7 and 8 of the murine eEF2K gene through the addition of a neomycin selection cassette. (**C)** eEF2K-/- mice were identified by PCR. (**D)** Western blot of eEF2K and p-eEF2 from eEF2K wild-type, heterozygous, and knockout mouse tissues. (**E)** Abolition of eEF2 phosphorylation in eEF2K-/- mouse tissues was confirmed by *in vitro* kinase assay in the presence of [γ-32P]-ATP. (**F**) Daily food intake for eEF2K+/+ and eEF2K-/- mice. (**G)** Weekly body weight increase after birth for eEF2K+/+ and eEF2K-/- mice. **(H)** Glucose tolerance tests. Wild-type mice (male, n=9) and eEF2K-/- mice (male, n=10) were fasted overnight before an IP injection of 2 g/kg glucose; blood glucose concentration was measured at indicated time points. **(I)** Insulin tolerance tests. Wild-type mice (male, n=9) and eEF2K-/- mice (male, n=10) were fasted for 5h before IP injection of 0.75 U/kg insulin and blood glucose concentration was measured at indicated time points. **(F-I)** Data are represented as mean +/- S.E.M. **(J)** The fraction of ovaries from postmenopausal female mice that possess antral follicles or corpora lutea. Results were based on the histology of serial ovarian sections, obtained from 17~21 month old females (9 wild type mice; 9 eEF2K-deficient mice). **(K)** Ovaries of 17-20 month old mice were serial sectioned and the number of large antral follcles with a healthy or unhealthy oocyte was counted. Irregular shaped oocytes or those with no nuclear staining were identified as unhealthy oocytes. eEF2K-/-, n= 19; eEF2K+/+, n=3. **(L-N)** Iron hematoxylin/aniline blue staining of ovary from 17-20 month old mice. Scale bars represent 50 μm. **(L)** Healthy oocyte with an oval shape and clear nuclear staining. **(M)** Unhealthy oocyte with an irregular shape and nuclear staining. **(N)** Unhealthy oocyte with no nuclear staining.

Chu Figure S3

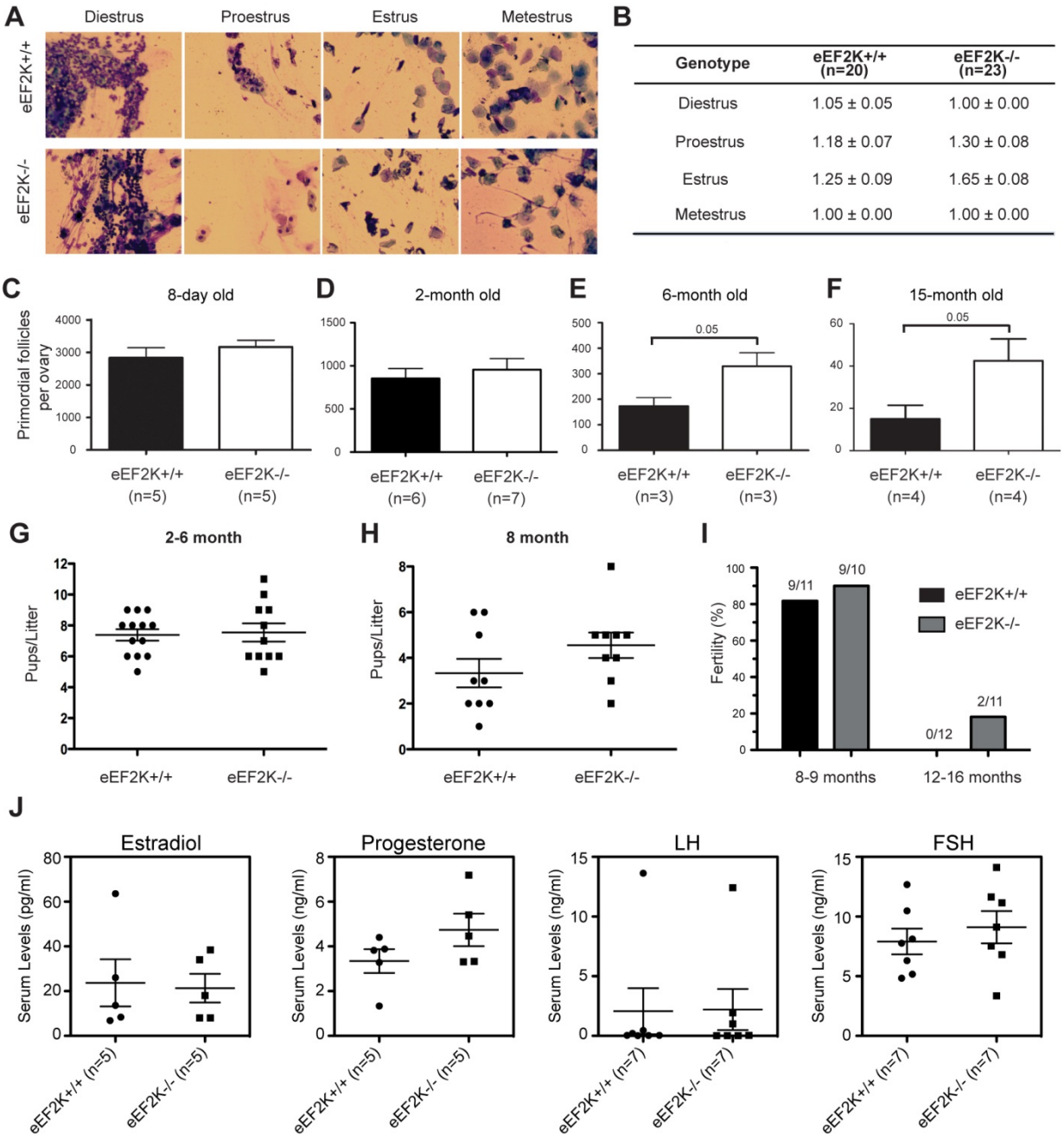

Genotype	eEF2K+/+ (n=20)	eEF2K-/- (n=23)
Diestrus	1.05 ± 0.05	1.00 ± 0.00
Proestrus	1.18 ± 0.07	1.30 ± 0.08
Estrus	1.25 ± 0.09	1.65 ± 0.08
Metestrus	1.00 ± 0.00	1.00 ± 0.00

Figure S3. Knockout of eEF2K delays estrus cycle progression and preserves primordial follicles in aged female mice, related to Figure 3. (A) Representative images of vaginal smears from female mice under different phases of the estrus cycle. **(B)** Duration of each phase of estrus cycle in days. Significant prolongation in estrus phase (Mann-Whitney *U*-test, two-tails, *P*=0.002) is shown. **(C-F)** Primordial follicle counts (**C**) 8-day old, (**D**) 2-month-old, (**E**) 6-month-old, and (**F**) 15-month-old eEF2K wild-type and knockout mice. Statistical significance (Mann-Whitney *U*-test, one-tail) is shown. **(G,H)** Pups number per litter for 2-6 month old and 8-month-old female mice. **(B-H)** Data are represented as mean +/- S.E.M. **(I)** Female fertility as the percentage of females who are able to be pregnant at the indicated ages. Female mice were mated with young (2-6 month old) wild-type males. **(J)** Hormone levels of estradiol, progesterone, LH and FSH were measured. Blood was collected from 3-month old females in estrus phase.

Chu Figure S4

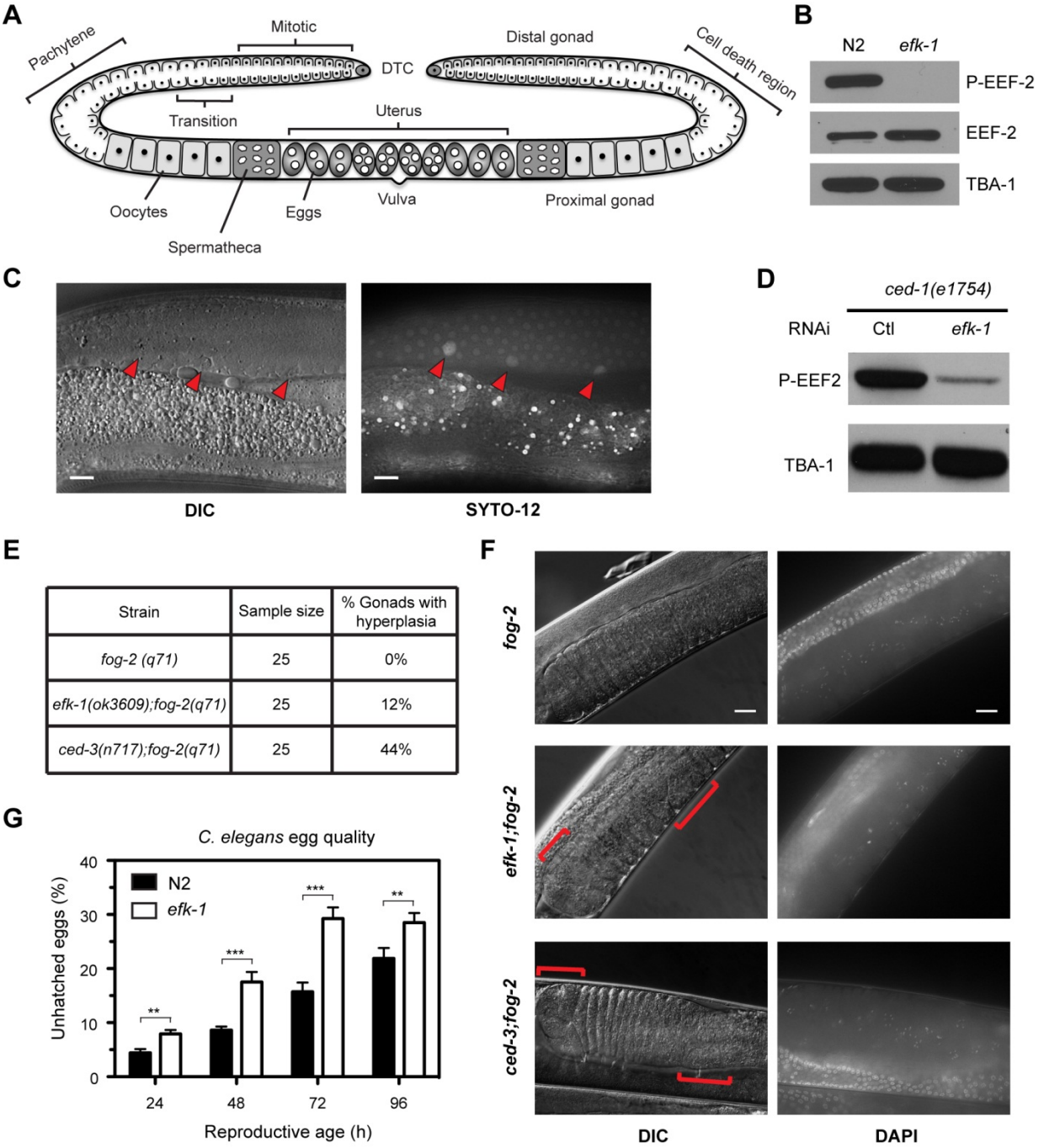

Strain	Sample size	% Gonads with hyperplasia
fog-2 (q71)	25	0%
efk-1(ok3609);fog-2(q71)	25	12%
ced-3(n717);fog-2(q71)	25	44%

Figure S4. Elongation factor 2 kinase functions to promote germ cell death and maintain germ cell quality in *C. elegans*, related to Figure 4. (A) Schematic representation of the hermaphrodite *C. elegans* gonad, showing the two U-shaped gonad arms joined at a central uterus. Shown are the distal tip cell (DTC), the distal gonad, including mitotic region, transition region, and pachytene/meiosis I region, and the proximal gonad, including maturing oocytes, spermatheca, and embryos, as well as the uterus and vulva. **(B)** Western blot analysis of N2 and *efk-1(ok3609)* for phospho-EEF-2, EEF-2, and TBA-1 (α-tubulin) in adult hermaphrodites. Phosphorylation of EEF2 is completely abolished in *efk-1(ok3609)* mutants. **(C)** Germ cell corpses observed by SYTO-12 staining and by Nomarski optics (shown by red arrowhead). Scale bars represent 10 μm. **(D)** Western blot analysis of P-EEF2 and TBA-1 (α-tubulin) in *ced-1(e1754)* mutants treated with control and *efk-1* RNAi. **(E)** Percentage of proximal gonads with hyperplasia amongst mature stacked oocytes. **(F)** DIC and DAPI-stained images for results shown for (E). Hyperplasia in the proximal gonad can be identified by red brackets. Scale bars represent 20 μm. **(G)** Hermaphrodites were subjected to 0.5% hypochlorite treatment at various stages of adult reproductive development in order to quantify the proportion of eggs that failed to hatch. For each time point, populations (>30 per genotype) of ~25-50 hypochlorite-treated eggs were used to calculate the percentage of unhatched eggs. Data are represented as mean +/- S.E.M. where ***<0.001, **<0.01, and *<0.05 (Mann-Whitney U-test).

Chu Figure S5

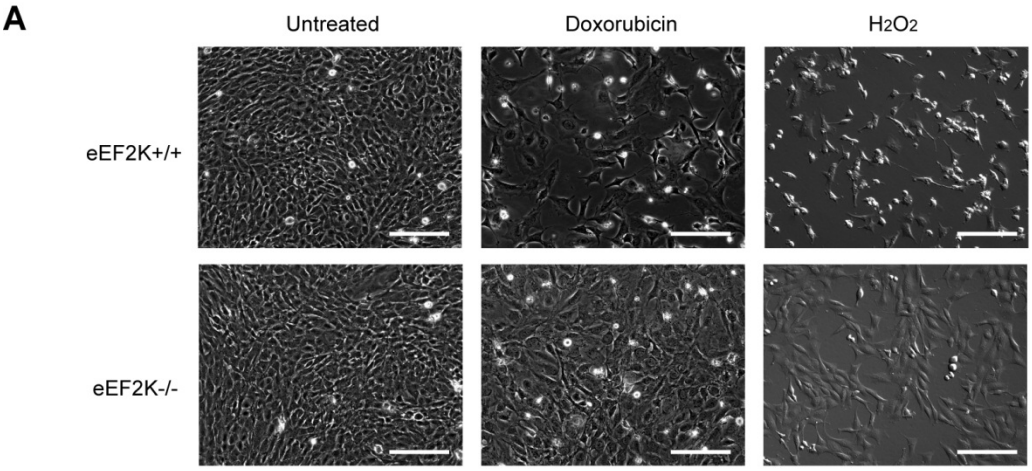

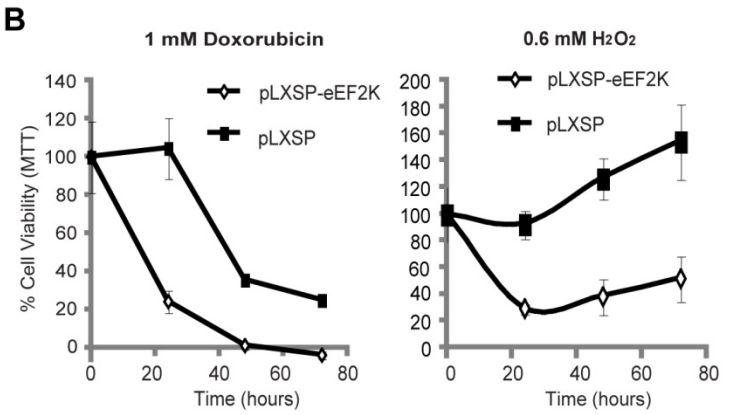

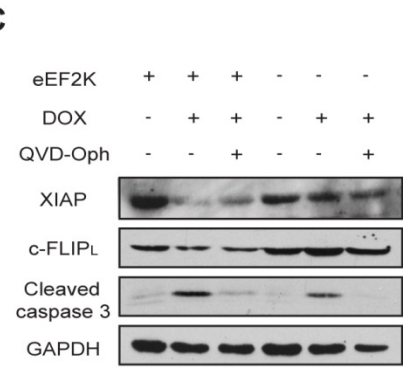

D

	% of total population
p-eEF2 positive staining	18.5 %
Condensed chromatin	17.5 %
TUNEL positive staining	15.2 %
	% of cells with condensed chromatin
p-eEF2 positive staining	84.9 %
	% of TUNEL positive cells
p-eEF2 positive staining	100 %

E

	% Protein synthesis		
MEFs	**-DOX**	**+DOX (6h)**	**+DOX (9h)**
pLXSP-eEF2K	100 ± 3.1	77.2 ± 6.1	53.6 ± 1.5
pLXSP	100 ± 2.1	79.4 ± 2.5	71.5 ± 5.3 **

Figure S5. Knockout of eEF2K suppresses apoptosis induced by oxidative stress in MEFs, related to Figure 5. (A) Phase-contrast images of cells. MEFs were treated for 24 hours with 1.6 μM doxorubicin or 400 μM hydrogen peroxide. Scale bars represent 50 μm**. (B)** MTT assay of eEF2K-/- MEFs expressing pLXSP empty vectors or eEF2K cDNA in pLXSP vectors treated with hydrogen peroxide or doxorubicin for different time periods. Data are represented as mean +/- S.E.M. **(C)** MEFs with or without eEF2K were treated with 1μM doxorubicin for 24h. Caspase activity was inactivated by adding the broad spectrum caspase inhibitor, QVD-OPh (20 μM), one hour prior to the doxorubicin treatment. Western blot shows that the protein levels of XIAP and c-$FLIP_L$ were not restored in QVD-OPh pre-treated cells. **(D)** TUNEL-positive cells contain intense phosphorylation of eEF2. HeLa cells were treated with 1.6 μM doxorubicin for 12h and stained for p-eEF2 and TUNEL staining. Condensed chromatin was visualized by DAPI staining. At least 300 cells were counted in each group. All cells with positive staining of TUNEL are also positive stained by p-eEF2. **(E)** Protein synthesis rate in eEF2K-/- MEFs infected with retrovirus containing eEF2K cDNA or empty vector pLXSP. Protein synthesis was measured during 3h periods following 6h or after 9h incubation with doxorubicin. The rate of protein synthesis was determined by estimating the $^{14}C/^{3}H$ ratios. Values are means ± SD, ** represents a significant difference where $P = 0.005$ (two-tailed *t*-test).

Chu Figure S6

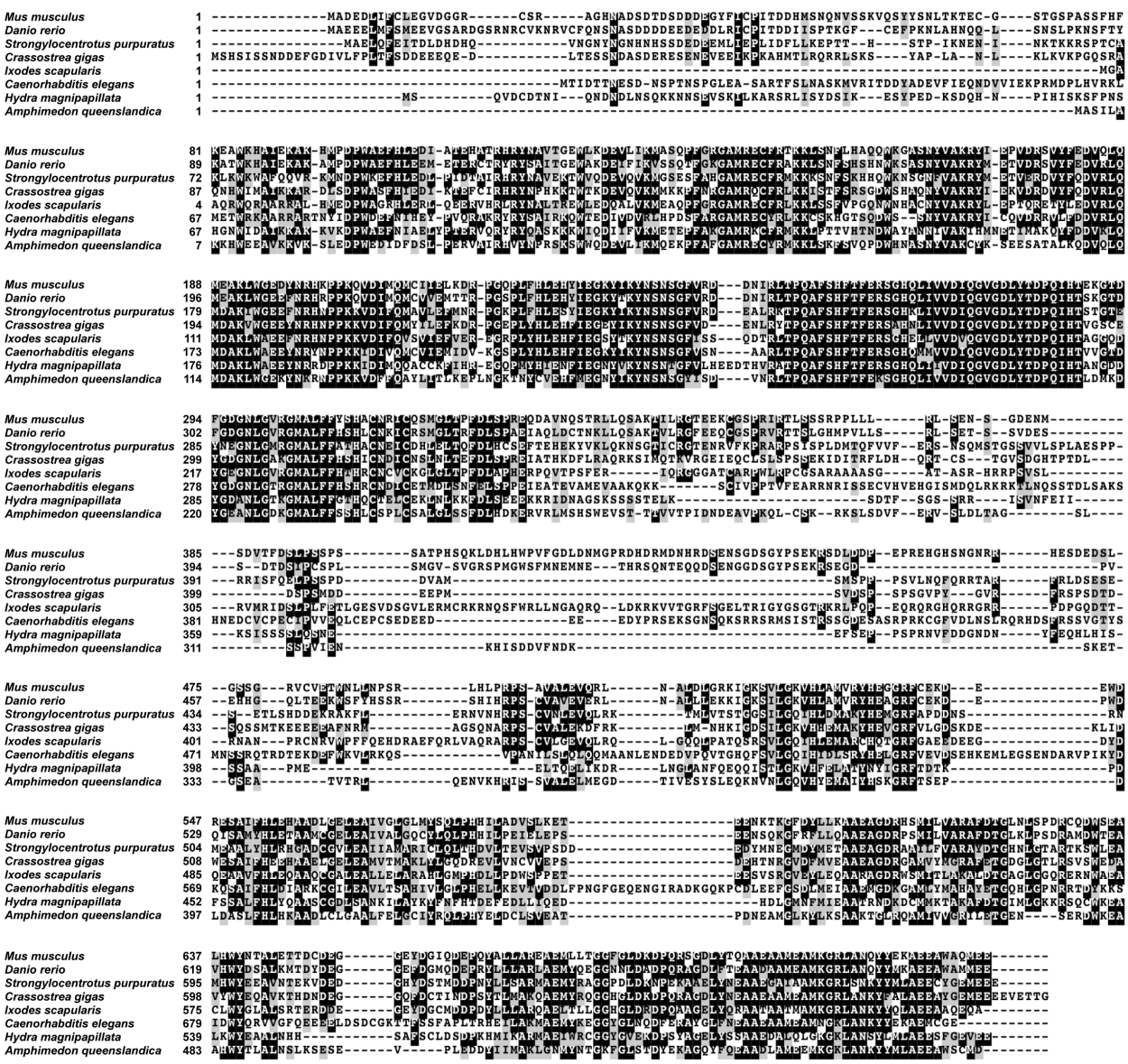

Figure S6. Elongation factor 2 kinase is conserved across eukaryotes, related to Figure 4. Protein alignment of elongation factor 2 kinase across diverse eukaryotes. Genbank accession numbers for protein sequences shown: *M. musculus*, AAH55361.1; *D. rerio*, AAH76410.1; *S. purpuratus*, XP_788087.1; *C. gigas*, EKC40554.1; *I. scapularis*, EEC15469.1; *C. elegans*, CCD65313.1; *H. magnipapillata*, XP_002162308.1; *A. queenslandica*, XP_003385502.1. Black shading indicates identical amino acids and gray shading indicates >50% consensus. Alignment performed via ClustalW algorithm and Boxshade 3.21.

Supplemental Experimental Procedures

The complete loss of eEF2 phosphorylation in eEF2K-/- mice.

To investigate the physiological role of eEF2K, we generated eEF2K-/- mice by disrupting the *Eef2K* gene in mouse embryonic stem cells. A targeting vector was used in which exon 7 and the majority of exon 8 of the *Eef2K* gene were replaced with the neomycin resistance gene (Figure S2A). This strategy resulted in elimination of a portion of the catalytic domain of eEF2K (Figure S2B). The mouse genotypes were analyzed by the PCR reactions (Figure S2C). The eEF2K+/- mice produced progeny of eEF2K+/-, eEF2K+/+ and eEF2K-/- mice with the expected ratio of 2:1:1. We analyzed the phenotype of eEF2K-/- mice and found that they were overtly normal, fertile and had a normal growth rate, food intake, and glucose and insulin tolerance tests (Figure S2F-I). Western blotting showed that no eEF2K protein was detected and no phosphorylation of eEF2 was observed in cell extracts from eEF2K-/- mice (Figure S2D). We also performed a kinase assay using purified rabbit eEF2 as a substrate and found that purified eEF2 was unable to be phosphorylated in eEF2K-/- cell lysates, indicating a complete lack of eEF2K activity in eEF2K-/- mice (Figure S2E).

Cell viability assay

For the MTT assay, $3*10^3$ cells/well (100 μl) were grown overnight in 96-well plates with DMEM containing 10% fetal bovine serum. Cell were treated with doxorubicin for 24h, then incubated with 20 μl of 1 mg/ml MTT (3-(4,5-dimethylthhiazol)-2,5-dipheyltetrazolium bromide) at 37°C for 4h. Media was removed and DMSO was added into each well. The number of viable cells was determined by measuring the absorbance at 550 nm.

Caspase inhibition by QVD-Oph

Pan-caspase inhibitor QVD-Oph [quinoline-Val-Asp(OME)-CH_2-PH] was purchased from

Calbiochem. When cells achieved a confluency of 70%, 20 μM QVD-Oph was added 30 min before the apoptotic stimuli. Consequently, cells were incubated in 1 μM doxorubicin (Sigma, MO) for 24h in the presence or absence of QVD-Oph to induce apoptosis. Cells were harvested and cell lysates were used for Western blotting analysis.

Analysis of mouse estrous cycle

Female mice were separated according to their genotypes. Vaginal smears were obtained every morning and stained with Giemsa stain (Sigma, MO). Light microscopy was used to identify the different stages of the estrous cycle based on smear cell morphologies. The approximate duration of each phase was estimated.

Hormone measurements

To measure hormone levels, estrus cycles were analyzed by vaginal smears in 3-month-old wild-type and eEF2K-deficient female mice. Mice were sacrificed on the estrus day and blood samples were collected by heart puncture. Whole blood samples were transferred into 1.5 mL centrifuge tubes and allowed to clot at room temperature for 90 min. Samples were centrifuged at 2,000g for 15 min, after which the serum was stored at -20°C. Mouse FSH-RIA, LH-IRMA, Progesterone-RIA, and Estradiol-ELISA assays were conducted by The University of Virginia Center for Research in Reproduction Ligand Assay and Analysis Core Facilities

Glucose and insulin tolerance test

For glucose tolerance test, 2-month-old eEF2K+/+ and eEF2K-/- male mice were fasted overnight, and IP injected with 20 mg/ml glucose at a dose of 2 g/kg body weight. For insulin tolerance test, mice were starved for 5h and IP injected with 0.75 U/kg body weight recombinant insulin (Invitrogen, CA). Blood was obtained from the tail at time points 0, 15, 30, 60, 120 min for glucose measurement.

Kinase assay

The eEF2 kinase assay was performed as described (Dorovkov et al., 2002). Mouse cell lysates were incubated with purified rabbit reticulocyte eEF-2 in reaction buffer (50 mM Hepes−KOH with pH 6.6, 10 mM magnesium acetate, 5 mM DTT, 100 μM $CaCl_2$, 0.5 μg calmodulin, 60 μM ATP, and 1 μCi [γ-^{32}P]-ATP (3000 Ci/mmol)). Reactions were incubated at 30 °C for 10 min and were terminated by incubation on ice with addition of Laemmli buffer. Samples were analyzed by 8% SDS−PAGE and autoradiography.

Measurement of protein synthesis with $^{14}C/^{3}H$ double labeling

For $^{14}C/^{3}H$ double labeling, $2*10^4$ fibroblasts/well were cultured in 12-well plate in the low leucine medium (L-leucine 6.6 mg/L) labeled with 5 μCi/ml of ^{3}H-Leucine for 24 hours. After the treatment with 1.6 μM doxorubicin for 6 hours or 9 hours in ^{3}H-labeled medium, cells were washed with PBS and were supplemented with ^{14}C labeled medium (2 μCi/ml of ^{14}C amino acids mixture) for another 3h. Subsequently, cells were lysed and radioactivity was determined as previously described (Dorovkov et al., 2002). The rate of protein synthesis was determined by calculating $^{14}C/^{3}H$ ratio.

Supplemental References

Dorovkov, M.V., Pavur, K.S., Petrov, A.N., and Ryazanov, A.G. (2002). Regulation of elongation factor-2 kinase by pH. Biochemistry *41*, 13444-13450.